

Wear Evaluation on Ni₃Al/MnS Composite Related to Metallurgical Processes

Karin Gong¹, LUO He-li², ZHOU Zhi-feng³, TIAN Zhi-ling²,
Lars Nyborg¹, LI Chang-hai¹

(1. Department of Materials and Manufacturing Technology, Chalmers University of Technology, Gothenburg Se-412 96, Sweden; 2. China Iron and Steel Research Institute Group, Beijing 100081, China; 3. Department of Manufacturing Engineering and Engineering Management, City University of Hong Kong, Hong Kong, China)

Abstract: Iron alloyed Ni₃Al with composition of Ni-18.8Al-10.7Fe-0.5Mn-0.5Ti-0.2B in atom percent (NAC alloy) showed attractive tribological properties under unlubrication condition at room temperature. The alloy was prepared by hot isostatic pressing (HIP) process. The wear properties were associated with its intrinsic deformation mechanism. Unfortunately, the single phase NAC-alloy worked inadequately with its counterpart disk, and also showed a poor machinability. In the present work, NAC-alloy matrix composite with 6% (volume percent) MnS particle addition was studied to improve its wear behaviors and performance on machining. Two metallurgical processes of HIP and vacuum casting were applied to produce the testing materials. Pin-on-disk (POD) measurements were carried out at room temperature. A commercial vermicular graphite cast iron was selected as a reference material. The counterpart disk was made of a grey cast iron as liner material in ship engines. The contact pressures of 2.83 MPa and 5.66 MPa were normally applied in the tests. The investigation indicated that MnS particle addition in the NAC-alloy composites functions as an effective solid lubricant, and improved wear properties and machinability of the materials. Obviously, as-cast NAC-alloy with in-situ formed MnS-phase was working more effectively with the counterpart, comparing to the HIPed NAC-alloy composite with MnS particles. At the high contact pressure of 5.66 MPa, the specific wear rate of the as-cast NAC-alloy composite was high. The phenomenon of the negative effect is mostly due to the brittle second NiAl phase as evidenced in the microstructure analysis.

Key words: HIP processing; friction coefficient; specific wear rate; intermetallics; sliding wear; casting; machinability

The advanced engines require increasingly high working temperatures, running speeds and loads. Therefore, there is a great interest to develop and test new materials. One of the candidates is the intermetallic materials. The main driving force for such research into intermetallics has in the past been their attraction for high temperature structural applications. It is only in a few of cases that their tribological properties have been studied. And therefore, there is ample scope in this area for fruitful further research, based on the intrinsic characters of the intermetallics. Especially, the tribological performances of Ni₃Al based alloys are the mostly attractive and studied in the intermetallic groups.

The intermetallic materials have long-range ordered crystalline structures with strong oriented atomic

bonding, which should be considered as a benefit to a slow wearing rate of the materials. They also show strong strain-hardenability and yield strength; even the strength is increased with raised temperature up until a certain level. In certain cases, these properties lead to excellent tribological properties under a certain temperature range. In fact, a number of laboratory studies have indicated that Ni₃Al based alloys have significant potential in wear critical applications, especially in cavitations erosion and sliding wear in the temperature range of 400–650 °C^[1–6]. In earlier works^[7–8] the scuffing resistance, friction coefficients and specific wear rates of an existed Ni₃Al based NAC-alloy with composition of Ni-18.8Al-10.7Fe-0.5Mn-0.5Ti-0.2B (atom percent, %) was investigated by Pin-on-disk (POD) test method for

Foundation Item: Item Sponsored by Swedish VINNOVA and Chinese MOST for International Collaborative Research Projects (P32737-1, P32737-2)

Biography: Karin Gong(1963—), Female, Doctor; **E-mail:** karin.gong@chalmers.se; **Received Date:** February 14, 2011

an initial understanding sliding wear behavior of the materials under unlubricated condition. Comparing to a commercial vermicular cast iron in ship engines, the selected single phase NAC-alloy has obtained the similar values of friction coefficient and specific wear rate. The wear mechanisms may conduct to its intrinsic deformation mechanism of the Ni₃Al type of intermetallics.

It was considered that the soft MnS particles shall act as a solid lubricant of the material. Therefore, a NAC-alloy composite with 6% (volume percent) MnS particle addition will be studied in the present work for improving wear performance of the Ni₃Al based materials.

Furthermore, machinability of the Ni₃Al alloy was expected to be improved by MnS addition. Ni₃Al has high tendency of strain hardening. With the effect of this, when machining, it shows adherence of workpiece Ni₃Al material to the cutting edge of the tool, resulting in a poor machinability. By adding MnS particles to the material one can avoid adherence of the material. The crack initiation can start from MnS particles when shearing of the material takes place in machining. Hence it can enhance machinability of Ni₃Al alloy.

HIP and vacuum casting processes were applied to prepare the testing materials. It was assumed that the HIP process will create a desirable phase constitution and microstructure of the testing materials. The casting process will be more operable for industries to produce some specified components, like the piston rings of heavy duty ship engines.

In the work, the prepared materials will be evaluated on wear behaviors related to their microstructures and the applied metallurgical processes.

1 Experimental Procedures

1.1 Materials selection for testing

From the previous works^[9-11], it has suggested that the sliding wear of metals commonly includes the following sequence of events: large plastic strains resulting from asperity contacts, generation of a heterogeneous substructure consistent with large strains, shear instability leading to transfer of material from one sliding component to the other, mechanical mixing which produces an ultra-fine grain size material on the surface, and removal of this mechanically mixed material as wear debris particles. Therefore, mechanical properties are very important related to the wear behaviour and machinability of materials. Especially, the strength of ma-

terial and its work hardening behaviour to plastic flow will control the extent of plasticity in the contact region. Certainly, the resistance to brittle fracture can lead to completely different mechanisms of wear from those dominated by plastic flow.

In the work, the NAC-alloy was selected as matrix of the HIPed and as-cast composites. In the principle, as a main alloying element, the solid solubility of Fe in Ni₃Al compound can reach 15% (atom percent). In the crystal, Fe atoms will replace Ni atoms or Al atoms in equal. Moreover, it can improve ductility and machinability^[7] by means of the addition of iron with the amount less than 11% (atom percent). Clearly, the production cost of the alloy will be decreased by adding Fe content. Ti has a similar electronic structure of aluminium; therefore it can replace Al and induce solid solution strengthening. Mn element is also used for strengthening. Boron is essential to improve room temperature ductility by increasing grain boundary cohesiveness. Several works^[12-13] revealed that the enhancement of mechanical properties by B addition improved tribological properties of Ni₃Al based alloys obviously. The as-cast composite with the composition of Ni-18.8Al-10.7Fe-1.2Mn-0.7S-0.5Ti-0.2B (atom percent, %) was designed. The testing material with 1.2% of Mn and 0.7% of S (atom percent) by calculation which produced by casting process will contain MnS phase no less than 6%. The matrix should have a very close composition as the original NAC alloy.

It is well known that the vermicular graphite cast iron has an optimized phase constitution and microstructure for its acceptable wear resistance by ship engine industries. Therefore, a commercial vermicular graphite cast iron was used as a reference material in this work for evaluating the testing materials. The disks applied in the work were made of a grey cast iron, as liner material in ship engines. Then, the measured results of the testing materials by tribological tests in this investigation can be conducted to certain industrial applications.

1.2 Materials preparation

The powders of NAC-alloy for HIP process were prepared by using plasma rotating electrode process (PREP). The PREP system was firstly evacuated up to 0.1 bars to prevent the formation of oxidation of the powders. The chamber was then flooded with inert gas of helium and argon. The electrode rod of the master alloy was rotated with a speed of 14500 ± 500 r/min. Then, an argon/helium plasma arc was

ignited. The plasma jet melted the tip of the rotating rod. A fusion film was formed on the front end of the rod, which disintegrated into small liquid metal droplets as a consequence of the centrifugal force. Due to surface tension the droplets are spherical. On their trajectories towards the chamber wall the droplets solidified rapidly in the inert atmosphere and formed spherical powders. The collected powders were sieving to a size range of 45 to 120 μm . The utilized MnS powders for preparing the HIPed composite have the same size range. A composite of NAC-alloy with addition of 6% (volume percent) MnS particles and a monolithic NAC-alloy were finally prepared by HIP process. The applied process data for HIP process are 1130 to 1160 $^{\circ}\text{C}$ as heating temperature under 140 MPa for 3 h. The densities of NAC-alloy and MnS particles used for calculating compositions of the composites in volume percentage are 7.25 and 3.99 g/cm^3 , respectively. The as-cast NAC-alloy composite with in-situ formed MnS particles was produced by using a vacuum (33×10^{-2} Pa) induction melting furnace in CISRI. The process holding temperature of melt is around 1550 $^{\circ}\text{C}$, and the pouring temperature is 1460 $^{\circ}\text{C}$ for the vacuum investment casting into a ceramic shell.

1.3 Materials characterization

The testing samples were analyzed by X-ray diffraction spectrometry. The equipment of D8 advance X-ray diffractometer analysis was performed on the HIPed monolithic NAC-alloy and its composites. The $\text{CrK}\alpha_1$ X-ray radiation (wavelength 0.228970 nm) was used to obtain the diffraction pattern and identify the phase constitution of the materials. A LEO 1550 Gemini scanning electron microscope (SEM) equipped with Oxford energy dispersive spectrometer (EDS) was utilized to evaluate quality of the testing samples. The backscattering electron image technique of SEM based on a composition contrast principle and the quantitative analysis of smart map EDS were applied to investigate microstructures and identify the phase constitution. In order to evaluate as-cast composite for a relevant industrial application, the mechanical properties of the as-cast composite will be measured in the work. The mechanical properties of as cast NAC-alloy composite were obtained by tensile test in the series of temperatures. The collected data included the ultimate strength, yield strength, elongation and area reduction of the material. A servo hydraulic Instron 3369 load frame equipped with a temperature chamber was used. The tensile speci-

mens were taken from the central area of a casting pot, and machined with the tensile direction perpendicular to axis of the ingot. The initial reference lengths of the samples are 25 mm. The strain rate is 1 mm/min. The tests were running in strain rate control and a clip-on extensometer was used to record the strain data during the deformation. The tensile tests were carried out in 20, 200, 400, 600 and 800 $^{\circ}\text{C}$ working conditions. Three of each testing samples were performed in the selected temperature range in order to obtain statistical result. The results from the analytical works were coupled to the experimental data from the tribological tests for evaluating and understanding wear behaviors of the studied materials.

1.4 Tribological tests

For evaluating friction coefficient and wear rate of different materials, a conventional pin-on-disk tribometer (Teer Coatings Ltd, UK) was used. The pins ($\phi 3$ mm \times 16 mm) of testing materials and the selected grey cast iron disks ($\phi 30$ mm \times 4 mm) as counterpart were machined to a surface roughness of less than 0.2 μm . The tests were performed under applied normalizing loads of 20 N and 40 N, corresponding to the contact pressure of 2.83 MPa and 5.66 MPa, respectively. The sliding speed of 0.08 $\text{m} \cdot \text{s}^{-1}$ was selected as a constant value by adjusting the rotation speed of the disk and the diameter of the wear track, and the duration of sliding time lasted for 6 h. The measurements were carried out at room temperature in laboratory air with a relative humidity of about 45%. For each specified wear couple, the wear test was at least repeated three times in order to obtain statistical testing results. Wear volumes of the pin samples were calculated from a mass loss method by assuming a density of 7.25 g/cm^3 for NAC alloy and 7.12 g/cm^3 for NAC-alloy matrix composite reinforced by 6% (volume percent) MnS particles. The density of the compact cast iron used for calculation was 7.30 g/cm^3 . Wear volumes of the disks were measured accurately by using a computerized three-axis profilometer (Taylor Hobson-PGI). The measured results on wearing in this work are reported in terms of Archard's specific wear rate R_{sw} ($\text{mm}^3 \cdot \text{N}^{-1} \cdot \text{m}^{-1}$), calculated by the following formula:

$$R_{\text{sw}} = V / (F \cdot S) \quad (1)$$

where, V is the volume worn away, mm^3 ; F is the applied normal load, N; and S is the sliding distance, m.

2 Results

2.1 Analytical works

The designations of the testing specimens are summarized in Table 1. Fig. 1 illustrates the backscattering electron images of the specimens. As shown in the images, the HIP testing materials obtained almost full density. In addition, it can be clearly seen that the phase morphologies of specimens 1, 2 and 3 are largely various, as shown from Fig. 1 (a) to (c). It is seen that specimen 1 has a single Ni₃Al phase microstructure. And in the HIPed composite, the reinforced MnS particles are well bonded to the matrix and homogeneously distributed. The in-situ

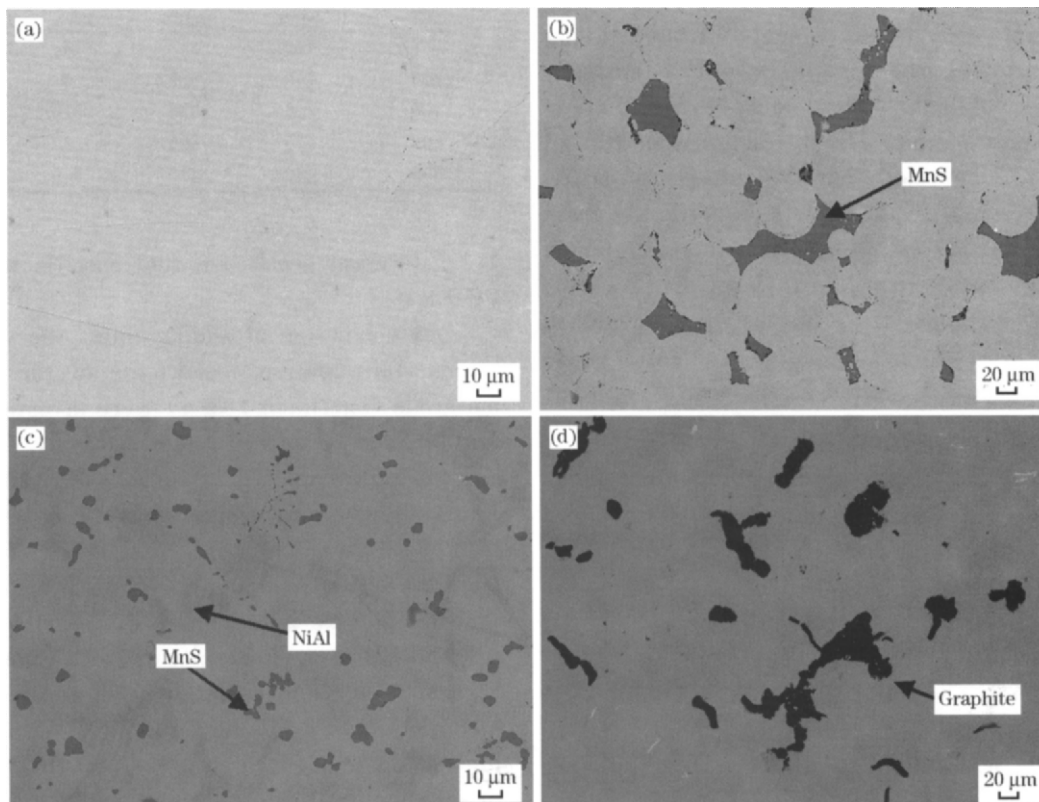
formed sulfide phase in as cast NAC-alloy composite can be clearly identified with a similar volume percentage as observed in the HIPed specimen 2. The in-situ formed phase is small and distributed homogeneously on the matrix. In Fig. 1 (d) a non-etched micrograph of the commercial vermicular graphite cast iron is given. The graphite phase with vermicular morphology was recognized.

The phases of specimens 2 and 3 were further identified by smart map EDS analysis, and the collected data are given in Table 2. The in-situ formed sulfide phase in the as-cast composite 3 was identified by EDS. It is important to notice that a high Al content second phase was also detected in the specimen. The Al

Table 1 Designation of pin and disk testing specimens

Designation	Composition	Process	Density/(g · cm ⁻³)
Pin specimen 1	Single phase NAC-alloy	HIP	7.25
Pin specimen 2	NAC-alloy+6% MnS	HIP	7.12
Pin specimen 3	NAC-alloy+in-situ MnS	Casting	7.12
Pin specimen 4	Vermicular cast iron ¹⁾	Casting	7.30
Disk	Grey cast iron ²⁾	Casting	7.30

Note: 1) The composition of vermicular cast iron in mass percentage as: C 3.05, Si 1.20, Mn 0.85, P 0.10 ± 0.05, S 0.05, Mo 0.65 ± 0.05, Cu 0.9 ± 0.05, V 0.02, Ti 0.03; 2) The composition of grey cast iron in mass percent as: C 3.2, Si 1.1, Mn 0.8, P 0.2, S 0.1, B 0.02, Cu 1.0, V 0.22.



(a) Specimen 1; (b) Specimen 2; (c) Specimen 3; (d) Specimen 4.

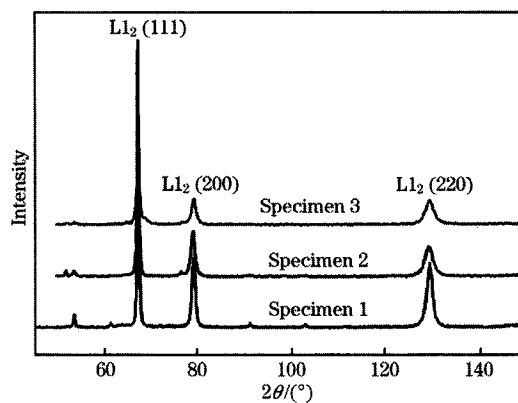
Fig. 1 Backscattering electron images of specimen 1 to 4

Table 2 Chemical composition analysis by EDS on specimen 2 and 3

			Ni	Al	Fe	S	Mn	Ti	Cr	C	Ca
Specimen 2	Matrix	Mean	69.72	16.36	11.36	0	0.75	0.58	0	1.23	0
		Standard deviation	2.11	0.64	0.33	0	0.06	0.11	0	3.02	0
	MnS particles	Mean	1.08	0	0.86	43.63	44.71	0	9.73	0	0
		Standard deviation	0.32	0.27	0	2.30	2.70	0.14	0	3.91	0
Specimen 3	Matrix	Mean	66.43	16.08	15.89	0	0.24	0	1.27	0	0.08
		Standard deviation	1.17	0.67	1.10	0	0.27	0	0.11	0	0.19
	MnS particles	Mean	1.08	0	0.86	43.63	44.71	0	9.73	0	0
		Standard deviation	0.29	0	0.18	0.76	2.37	0	1.49	0	0
	Second phase	Mean	59.52	27.83	11.52	0	0.54	0	0.60	0	0
		Standard deviation	0.50	0.41	0.17	0	0.08	0	0.11	0	0

content in the second phase was much higher than the average Al content in the NAC alloy. In the contrast, the relevant Ni content in the phase was quite low, compared to the Ni content of the named composition of NAC-alloy. The Fe content in the second phase was also relevant lower than that in the NAC-alloy matrix.

For determining the phase constitution of the specimens prepared by HIP and casting processes, XRD analysis was carried out, and the spectra of specimens 1, 2, and 3 were collected and presented in Fig. 2. In specimen 1, there is only one phase which can be identified by the relevant spectrum, i. e. a Ni_3Al type (L1_2) crystal structure with the main peak at $2\theta = 67.1^\circ$, derivative of the face centered cubic (fcc) crystal. Combining the results from EDS analysis, the monolithic NAC-alloy should be a $(\text{Ni}, \text{Fe})_3(\text{Fe}, \text{Al})$ intermetallic compound. The diffraction spectrum of the specimen 2 revealed that two phases of Ni_3Al matrix and the added MnS particles with the main peak at $2\theta = 51.99^\circ$ existed in the material, which were also coincident with the EDS analysis. As indicated by EDS analysis, three phases were recognized in specimen 3. They are Ni_3Al phase, MnS phase and NiAl phase which should be the high Al content phase.

**Fig. 2** XRD-spectra of testing specimen 1, 2 and 3

Ultimate strength, yield strength, elongation and area reduction of specimen 3 by tensile tests were collected in Table 3. As an intrinsic character of Ni_3Al type alloys, the as cast NAC-alloy with in-situ formed MnS particles showed an anomalous strength relevant with temperature, especially the yield strength was raised with increasing temperature obviously. The effect phenomenon was maintained up to 600°C .

Table 3 Mechanical properties of specimen by tensile tests

Testing temperature/ $^\circ\text{C}$	Ultimate strength/ MPa	Yield strength/ MPa	Elongation/ %	Area reduction/ %
20	710	—	5	8.5
200	740	565	8	12.5
400	700	645	5.5	7.5
600	690	595	5	10
800	470	410	5.5	7.5

2.2 Friction coefficient and specific wear rate in POD test

As a function of sliding time, the variations of steady-state friction coefficients of the testing pin materials (specimen 1 to 4) were investigated under two loads of 20 and 40 N, respectively. The collected data indicated that the tested materials (specimen 1 to 4) have a measurable friction coefficient under a load of 20 N; unfortunately, the recorded data of the friction coefficient under 40 N was outside the upper limit of the load cell during sliding time at the beginning of the test. It resulted in the tests under the high load of 40 N interrupted the measurement immediately. Only one exception for pin No. 2 under high load of 40 N was observed that the friction coefficients was sufficiently lower than the friction coefficients obtained under the load of 20 N. Thereafter, a load of 20 N was finally applied to determine the relevant values of friction coefficient from the differ-

ent tested specimens in this work. The statistical data are illustrated in Fig. 3. It can be reliable to see that both of MnS phase containing specimen 2 and 3 have a similar function to reduce friction coefficients, compared to the HIPed monolithic NAC alloy No. 1 without MnS addition. Clearly, in the group, as-cast NAC-alloy with in-situ formed MnS phase has the lowest friction coefficient comparing with the others.

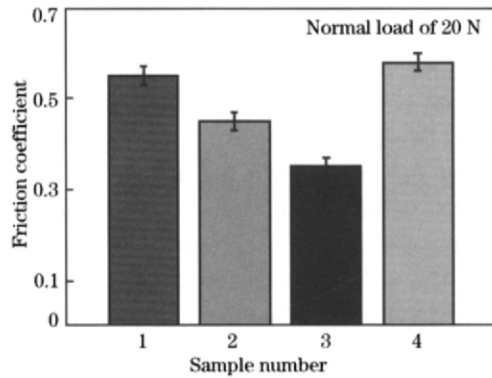


Fig. 3 Friction coefficients of testing samples 1 to 4 under load of 20 N

The specific wear rates of the tested pin materials were performed and carried out under the normal loads of 20 N and 40 N for unlubricated condition. The calculated values of specific wear rates of the pins are illustrated in Fig. 4. Of the specific wear rate of the pin in the high load of 40 N, specimen 1 and 2 are almost the same value and they are close to the commercial vermicular cast iron No. 4 under the load of 40 N. However, the specific wear rate of the as cast NAC-alloy with the in-situ formed MnS phase (specimen 3) had been the order of magnitude of five times worse than others. Unfortunately, there is not a several variation of the testing data under the lower load of 20 N. It was also noticed that the HIPed composite No. 2 showed a higher specific

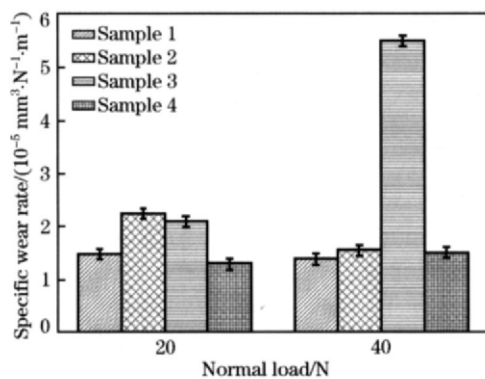
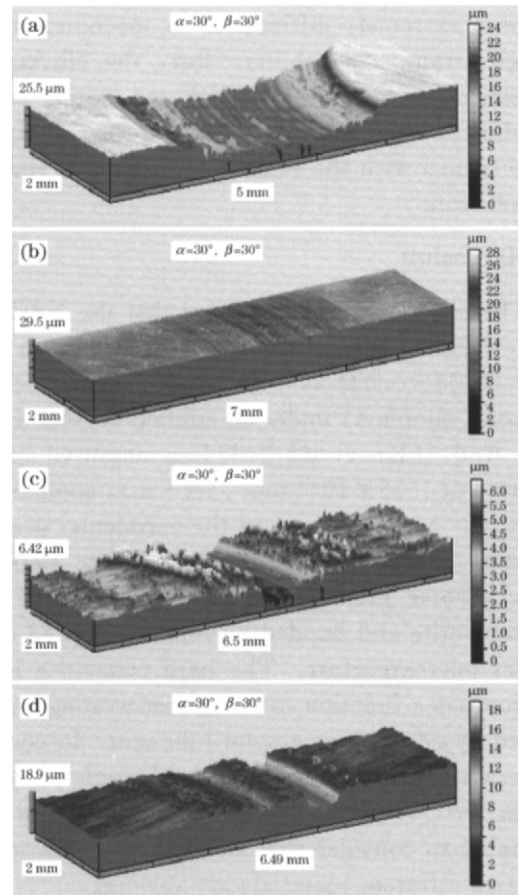


Fig. 4 Specific wear rates of testing samples 1 to 4 under loads of 20 and 40 N

wear rate in the load of 20 N, comparing to its specific wear rate under the load of 40 N.

Fig. 5 shows the 3-D images of the wear tracks of the disks after the wear tests under a load of 40 N. The calculated specific wear rates of the disks were given in Fig. 6. Pin No. 1 revealed the worn surface of the relevant disk material seriously. The worn surface of the disk countered to specimen 2 was smooth with a few



(a) Disk 1; (b) Disk 2; (c) Disk 3; (d) Disk 4.

Fig. 5 3-D profile images of worn surface of disks under load of 40 N

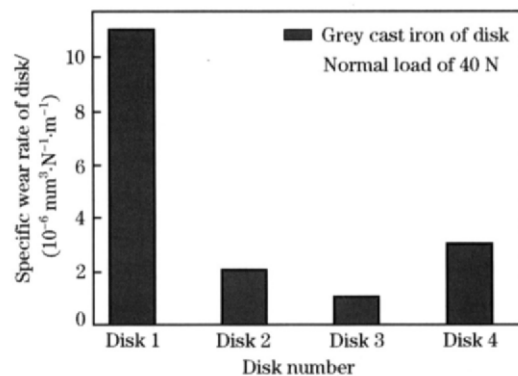


Fig. 6 Specific wear rates of disks against testing pin materials (No. 1 to No. 4) in 40 N loads

friction tracks, compared to the disk against pin No. 3, although pin No. 3 caused a lowest wear rate on the disk. In general, MnS addition has effectively reduced wearing on the counterparts, and resulted in a lower specific wear rate of the disks than the reference vermicular cast iron induced.

2.3 Tests on machining

Simple tests revealed that the monolithic NAC-alloy was extremely difficult to be machined due to its high strain-hardenability. But, the Ni₃Al/MnS composites, prepared by both HIP and casting processes, showed significantly improved machinability, can be turned with the same process data of the normal cast iron.

3 Discussion

The pin-on-disk tests revealed that the NAC-alloy sample 1 has an almost same measured friction coefficient (0.55 ± 0.02) as 0.58 ± 0.02 of the reference cast iron (sample 4) under an applied normal load of 20 N. And, it has even a little less measured specific wear rate of $1.38 \times 10^{-5} \text{ mm}^3/(\text{N} \cdot \text{m})$, compared to $1.50 \times 10^{-5} \text{ mm}^3/(\text{N} \cdot \text{m})$ of the vermicular graphite cast iron. It was known that the pearlite matrix of the vermicular graphite cast iron consists of very hard cementite and bonded by ferrite, formed a fine lamellar microstructure. The hard cementite in the cast iron has a function to be against wearing mostly, assisted by graphite as a solid lubricant. In contrast to the cast iron, there is only Ni₃Al single phase existed in NAC-alloy sample 1. Therefore, it will be reasonable to consider that the wear mechanisms of these two different materials are various.

The wear behaviour of Ni₃Al type alloys may relate to their intrinsic characters on deformation. The measured data of mechanical tests of this work revealed that the yield strength of the tested specimen 3 was anomalously increased due to the raised temperatures. This anomalous dependence of yield strength and temperature is a character for L1₂ type of intermetallics. The phenomenon can be explained by superdislocation movement in the ordered alloys. The deformation mechanism of superdislocation movement in long-range ordered alloys makes them having much higher strain-hardenability than in disordered alloys. The peaks of the strain hardenability are usually exhibited at intermediate temperatures. It has been suggested that the high hardening rate in the ordered crystals may be due to the generation of antiphase domain boundary (APB) tubes formed by

cross slip pinning^[14-15]. The APB and/or stacking fault energy of different lattice plans in the ordered structures will be changed by temperatures. When the difference is getting less, the cross-slipping of the screw dislocations will occur more easily and finally resulted in high strain-hardenability. It is believed that a hard layer on the NAC-alloy was formed quickly due to its high strain-hardenability at the beginning of friction, and led to the lower specific wear rates of the HIPed monolithic NAC alloy No. 1 and its composite No. 2 under a higher load of 40 N, compared to the data from the load of 20 N testing condition. Previous studies^[8,16-17] also indicated that the relative hardness of the pin and disk is one of the key factors, which influence the wear behaviour of the counterparts. The induced hard surface layer will wear the soft counterpart quickly, and also due to abrasive wearing by severe deformed hard debris particles.

Soft MnS particles were considered as a solid lubricant and added into Ni₃Al alloy. Hardness of HV_{100 g} 333 of MnS is less than hardness of HV_{100 g} 402 of the NAC-alloy. It was recognized that the addition of MnS into NAC-alloy will be beneficial to both wear counterparts. In fact, the added 6% (in volume percent) MnS particles reduced friction coefficient of the HIPed composite No. 2 to a value of 0.45 ± 0.02 . The as-cast NAC alloy No. 3 with in-situ formed MnS-phase has even lower friction coefficient of 0.35 ± 0.02 . The MnS particles in the sample 2 reduced the specific wear rate of its counterpart disk to $2.07 \times 10^{-6} \text{ mm}^3/(\text{N} \cdot \text{m})$, compared to a specific wear rate of the disk worn by the single phase pin No. 1 [$11.01 \times 10^{-6} \text{ mm}^3/(\text{N} \cdot \text{m})$]. And, the sample of No. 3 in the intermetallic material group was most friendly worked with the counterpart, having a specific wear rate of $1.07 \times 10^{-6} \text{ mm}^3/(\text{N} \cdot \text{m})$ of the disk. Probably, it is due to the small size of in-situ formed MnS particles and NiAl phase in the materials. The analytical work revealed that there is a NiAl phase existed in the as-cast material sample 3. Measured specific wear rate of the sample is $5.48 \times 10^{-5} \text{ mm}^3/(\text{N} \cdot \text{m})$, worse than $1.54 \times 10^{-5} \text{ mm}^3/(\text{N} \cdot \text{m})$ of sample 2. The research works by J H Jin et al^[18-20] pointed out that NiAl single phase alloys are brittle. The sliding wear resistance of NiAl based alloys is one or two orders of magnitude worse, comparing to Ni₃Al based alloys, which is strongly related to their hardness and toughness due to the plastic deformation mechanism at the contact surfaces between the sliding pair. The authors' pre-

vious work^[21] also showed that NiAl based alloy has a worse wear performance than the Ni₃Al based alloy. At the first step, the wear behaviour can be simply understood on a mixture regulation, which means that a less wear resistant NiAl phase increased specific wear rate of the material in practice. It should further consider that the fragment of the brittle NiAl phase as hard particles causes abrasion. Therefore, a single Ni₃Al phase matrix is preferable for a critical wear resistant composite.

The reason to form NiAl phase in the as-cast composite is due to fast cooling rate of the casting process. On the contrary, there are only Ni₃Al and MnS two phases existed in the HIPed composite. A slow cooling rate in the HIP process at a temperature range of 1100 to 500 °C resulted in an equilibrium microstructure. Obviously, the microstructure of the as-cast alloy is in an un-equilibrium condition, which was proved by the analytical result of XRD on the NAC-alloy powders^[7], and there is an even stronger {110} diffraction peak of the NiAl-phase in the spectrum than the peak from the as-cast alloy.

Finally, it was interesting to recognize that the as-cast NAC-alloy with not less than 6% (in volume percent) MnS-addition has yield strength over 550 MPa up to 600 °C. At the same time, the ductility of the material is practically acceptable for engineering applications. Also, the Ni₃Al/MnS composites can be machined as a normal industrial cast iron. Considering the much lower strength level of the existing cast iron, around 440 MPa under room temperature of a commercial product, for instance, and more serious requirement on mechanical properties of the wear resistant engine components, the as-cast NAC-alloy matrix composites can be further developed by improving metallurgical process to avoid NiAl-phase.

4 Conclusions

1) The single phase NAC-alloy prepared by HIP process in this work has a similar friction coefficient and specific wear rate under different testing conditions as compared to a commercial vermicular cast iron used in ship engines. However, during the sliding wear, the single phase NAC-alloy caused more severe wear on its grey cast iron counterpart. Therefore, the monolithic NAC-alloy material should not be applied to unlubricated wearing condition. It can probably be suitable as a matrix material to develop wear resistant composites. The wear behaviors are most probably conducted to its intrinsic deformation mechanism of the Ni₃Al type of intermetallics.

2) MnS particle addition in the HIPed NAC-alloy may function as an effective solid lubricant, and improve its friction coefficient against the grey cast iron disk, also decreased specific wear rate of the counterpart dramatically. However, its own specific wear rate remained as the same as the monolithic NAC-alloy.

3) As-cast NAC-alloy with the in-situ formed MnS phase worked almost better for the counterpart with a lower friction coefficient and specific wear rate, as compared to the HIPed composite. The specific wear rate of itself was high. The reason caused this negative effect is probably due to a brittle NiAl phase existed in the microstructure.

4) MnS particles addition in Ni₃Al-alloy obviously enhanced possibility to machine the material by normal cutting processes.

5) Casting process of the composite is economical and operable for producing some specified engine components, like piston rings. However, a faster cooling rate of casting process led to a non-equilibrium solidification of the material. To reach a desirable phase constitution and microstructure of the as-cast NAC-alloy composite, the relevant casting process should be further developed, especially on controlling solidification rate. Maybe, an additional thermo-treatment is needed.

Considering other excellent physical, chemical and mechanical properties of the Ni₃Al based intermetallic composite materials; the present investigation has recognized that it will be meaningful to develop Ni₃Al matrix composites for tribological utilization. The soft MnS particles are one of the hopeful reinforcement. Further investigations are needed on wear mechanism, influence of composition and microstructure on tribological performance of the alloy system, etc.

References:

- [1] Marquardt B J, Wert J J. Wear Induced Deformation of Ni₃Al, (Fe, Co)₃Al and (FeNi)₃V [J]. Proc Mater Res Soc, 1985, 39: 247.
- [2] Blau P J, DeVore C E. Sliding Behaviour of Alumina/Nickel and Alumina/Nickel Aluminide Couple at Room and Elevated Temperature [J]. J Tribology, 1988, 110: 646.
- [3] Bonda N R, Rigney D A. Unlubricated Sliding Wear of Nickel Aluminides at Room Temperature and 400 °C [J]. Proc Mater Res, 1989, 133: 585.
- [4] Blau P J, DeVore C E. Temperature Effects on the Break-in of Nickel Aluminide Alloys [C]//Proceedings of the 1989 Wear of Materials Conference. [S. l.]: American Society of Mechanical Engineers, 1989: 305.
- [5] Blau P J, DeVore C E. Sliding Friction and Wear Behaviour of

- Several Nickel Aluminide Alloys Under Dry and Lubricated Condition [J]. *Tribol Ins*, 1990(10): 226.
- [6] Johnson M, Mikkola D E, March P A, et al. The Resistance of Nickel and Iron Aluminides to Cavitation Erosion and Abrasive Wear [J]. *Wear*, 1990, 140: 279.
- [7] Gong Karin, Luo Heli, Feng Di, et al. Wear of Ni₃Al-Based Materials and Its Chromium-Carbide Reinforced Composites [J]. *Wear*, 2008, 265: 1751.
- [8] Gong Karin, Zhou Zhifeng, Shum P W, et al. Tribological Evaluation on Ni₃Al-Based Alloy and Its Composites Under Unlubricated Wear Condition [J]. *Wear*, 2011, 270: 195.
- [9] Rigney D A, Chen L H, Naylor M G S, et al. Wear Process in Sliding Systems [J]. *Wear*, 1984, 100: 195.
- [10] Rigney D A, Naylor M G S, Divakar R, et al. Low Energy Dislocation Structures Caused by Sliding and by Particle Impact [J]. *Mater Sci and Eng*, 1986, 81: 409.
- [11] Rigney D A. Adhesion Processes in Technological Application [J]. *Mater Sci and Eng*, 1986, 83: 189.
- [12] LA Pei-qing, XUE Qun-ji, LIU Wei-min. Effects of Boron Doping on Tribological Properties of Ni₃Al-Cr₇C₃ Coatings Under Dry Sliding [J]. *Wear*, 2001, 249: 94.
- [13] Yavuz Solmaz, Halidun Kelestemur M. Wear Behaviour of Boron-Doped Ni₃Al Material at Elevated Temperature [J]. *Wear*, 2004, 257: 1015.
- [14] Kear B H, Giamei A F, Leverant G R, et al. On Intrinsic/Extrinsic Stacking Fault Pairs in the LI₂ Lattice [J]. *Scripta Metallurgica*, 1969, 3: 123.
- [15] Kear B H. Dislocation Configuration and Work Hardening in Cu₃Au Crystal [J]. *Acta Met*, 1964, 12: 555.
- [16] Chiou Y C, Kato K, Abe H. The Effect of Normal Damping in the Loading System on the Wear of Low Carbon Steel [J]. *Wear*, 1987, 114: 73.
- [17] Akagaki T, Rigney D A. Sliding Friction and Wear of Metals Vacuum [J]. *Wear*, 1991, 149: 353.
- [18] Jin J H, Stephenson D J. The Sliding Wear Behaviour of Reactively Hot Pressed Nickel Aluminides [J]. *Wear*, 1998, 217: 200.
- [19] Miracle D B, Darolia R. Metal Matrix Composites—From Science to Technological Significance [J]. *Composites Science and Technology*, 2005, 65: 2526.
- [20] Kennedy F E, Hussaini I S Z. Thermo-Mechanical Anaysis of Dry Sliding Systems [J]. *Computers and Structures*, 1987, 26: 345.
- [21] Karin Gong. Tribological Properties of Ni₃Al-Based Materials [D]. Gothenburg: Chalmers University of Technology, Sweden, 2001.